

red Stress relaxation through crosslink unbinding

in cytoskeletal networks

C. Heussinger

Institute for Theoretical Physics, Georg-August-Universität Göttingen,
Friedrich-Hund-Platz 1, 37077 Göttingen, Germany

E-mail: claus.heussinger@theorie.physik.uni-goettingen.de

Abstract. The mechanical properties of cells are dominated by the cytoskeleton, an interconnected network of long elastic filaments. The connections between the filaments are provided by crosslinking proteins, which constitute, next to the filaments, the second important mechanical element of the network. An important aspect of cytoskeletal assemblies is their dynamic nature, which allows remodeling in response to external cues. The reversible nature of crosslink binding is an important mechanism that underlies these dynamical processes. Here, we develop a theoretical model that provides insight into how the mechanical properties of cytoskeletal networks may depend on their underlying constituting elements. We incorporate three important ingredients: nonaffine filament deformations in response to network strain; interplay between filament and crosslink mechanical properties; reversible crosslink (un)binding in response to imposed stress. With this we are able to self-consistently calculate the nonlinear modulus of the network as a function of deformation amplitude and crosslink as well as filament stiffnesses. During loading crosslink unbinding processes lead to a relaxation of stress and therefore to a reduction of the network modulus and eventually to network failure, when all crosslink are unbound. This softening due to crosslink unbinding generically competes with an inherent stiffening response, which may either be due to filament or crosslink nonlinear elasticity.

PACS numbers: 87.16.A-,87.16.Ln,83.50.-v

Submitted to: *New J. Phys.*

1. Introduction

Cells display complex nonlinear and time-scale dependent rheological properties [1, 2, 3]. A broad range of relaxation timescales results in power-law spectra for the frequency dependence of the linear viscoelastic response [4]. Under nonlinear loading conditions, cells can display apparently contradicting behaviors, ranging from fluidization to reinforcement [5, 6, 7]. Understanding these mesoscale behaviors in terms of underlying non-equilibrium processes, such as cytoskeletal remodeling, motor activity or reversible crosslink binding or folding, remains an important theme in current biomechanical research.

Over recent years, reconstituted f-actin networks have become a popular model system in which these phenomena can be studied in detail. Much of previous research in this field focused on the frequency-dependent rheology of *permanently crosslinked* filament networks [8, 9, 10]. Key questions revolve around the high-frequency modulus and its dependence on frequency ω [11, 12], the nature of network deformations (affine vs. non-affine) at intermediate frequencies [13, 14] and the nonlinear response properties of the network [15, 16]. Theoretical models [17, 18, 19] and simplified simulation schemes [20, 21, 22, 23, 24] have been proposed that aim at explaining one or the other of these non-trivial features.

In these studies, the filaments and their mechanical and thermal properties are assumed to dominate the effective rheology of the system. This may be different in F-actin networks crosslinked with the rather compliant crosslinking protein filamin. Experimental and theoretical work [25, 26, 27] suggest a second, crosslink-dominated regime, where network rheology is set by the crosslink stiffness, while filaments effectively behave as rigid, undeformable rods. In between these two extreme scenarios a proper treatment would have to consider the full interplay between crosslink and filament mechanical properties. This has not been addressed theoretically before.

Recent experiments have indicated that at low driving frequencies effects due to crosslink binding become important. This is evidenced, for example, as a peak in the loss modulus G'' [28] or a broad distribution of time-scales leading to an anomalous scaling with frequency, $G'' \sim \omega^{1/2}$ [29]. Theoretical modelling in this field are only beginning to emerge [30, 7, 29]. Some of the pertinent problems are: what is the force on a crosslink and how does it depend on network deformation? how does this affect binding? once unbound, how does this affect the network?

A noteworthy recent development is the phenomenological “glassy wormlike chain” model [31, 32]. In that approach, filament-filament interactions, as for example mediated by specific crosslinking, are not modeled explicitly, but are assumed to lead to an exponential stretching of the single filament relaxation times. Network deformation is accounted for by a pre-stretching tensile force in the filament. The same force is assumed to enter the unbinding rate constant of the crosslinks via a Bell-like model [7].

Here, we go beyond previous studies by investigating the interplay between filament and crosslink elasticity and its effects on the crosslink binding behavior. We will present a simple model that accounts for the individual crosslinks, their mechanical properties as well as their binding state. The model is a fully thermodynamic treatment, where crosslink binding is equilibrated for a given network deformation. No rate effects will be considered. As a result of our analysis, we will be able to selfconsistently calculate the nonlinear elastic modulus of the network, which incorporates as key ingredient the ensuing tendency for crosslinks to unbind under load.

The manuscript is structured as follows. In section 2 we will define our model and relate it to existing approaches in the literature. In the model the filament network is represented as an effective elastic medium with a given, fixed modulus k_m . We will introduce a Hamiltonian that describes the properties of a test filament embedded in this medium. In section 3 we will present results of Metropolis Monte-Carlo simulations for the Hamiltonian introduced. In section 4 a theoretical framework will be developed that allows some analytical results to be obtained. Finally, in section 5 we will discuss the question of how to obtain in a self-consistent way the stiffness of the effective medium in terms of the response properties of the test filament.

2. Model

We will consider the properties of a test filament crosslinked into a network. The filament is described in terms of the worm-like chain model. In “weakly-bending” approximation the bending energy of the filament can be written as

$$H_b = \frac{\kappa_b}{2} \int_0^L \left(\frac{\partial^2 y}{\partial s^2} \right)^2 ds \quad (1)$$

where κ_b is the filament bending stiffness and $y(s)$ is the transverse deflection of the filament from its (straight) reference configuration at $y_0(s) = 0$. In these expressions s is the arclength, $s = [0, L]$, and L is the length of the filament.

The effect of the surrounding network is to confine the test filament to a tube-like region in space. In this way the actual network is substituted by an effective potential that acts on the test filament. A convenient potential is the harmonic tube

$$V = \frac{1}{2} \int_0^L k(s)(y(s) - \bar{y}(s))^2 ds, \quad (2)$$

where $k(s)$ is the strength of the confinement and $\bar{y}(s)$ is the tube center, which may or may not be different from the reference configuration of the filament.

The tube potential is a convenient representation of many-body network effects on the test filament. However, the parameters entering the potential (here k and \bar{y}) and their relation to network deformation and mechanical properties are usually unknown. Ideally, these parameters can be determined in a self-consistent way from the analysis of the test filament.

In the following, we will present a theoretical framework, where such a self-consistent determination is partly possible (see Fig. 1 for a short description). In this model we assume the network to be represented by an effective medium that couples to the test filament only at the crosslinking points,

$$k(s) = k_\times \sum_{i=1}^{N_\times} n_i \delta(s - s_i) \quad (3)$$

where k_\times is the crosslink stiffness. N_\times is the total number of crosslinking sites. Being interested in the effects of reversible crosslink binding, we also include an occupation variable $n_i = 0, 1$. If the crosslink is bound at site i , we have $n_i = 1$, if it is unbound then $n_i = 0$. Below, we will also introduce (and calculate self-consistently) the modulus k_m of the effective medium. The crosslink stiffness k_\times in equation (3) then has to be substituted by an effective stiffness $k_{\text{eff}}(k_\times, k_m)$, which contains contributions from both, the crosslinks and the effective medium. For the time being we set $k_m \rightarrow \infty$ and thus $k_{\text{eff}} \rightarrow k_\times$.

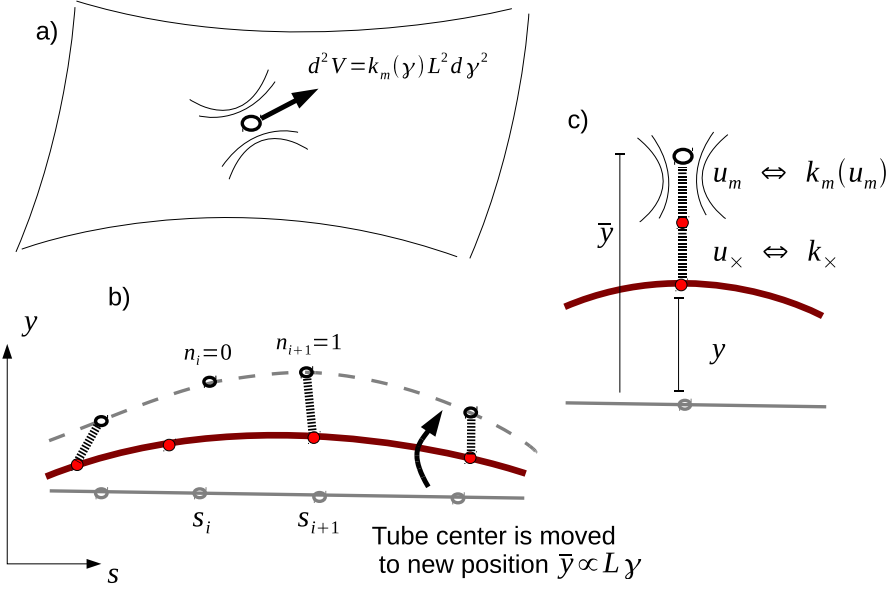


Figure 1. Illustration of the modeling assumptions. a) On a macroscopic level the filament network is modeled as a (nonlinear) elastic medium with modulus $k_m(\gamma)$. b) On the microscopic level the effect of the network is to confine the filament to a tube-like region in space. In a densely crosslinked network the tube potential mainly acts at the crosslinking sites $i = 1 \dots N_\times$, which are located at discrete points s_i along the filament axis and which may be bound ($n_i = 1$) or unbound ($n_i = 0$). A macroscopic strain γ leads to an inhomogeneous distortion of the effective medium, which is accounted for by a shift of the tube center line, $\bar{y} \propto L\gamma$ (dashed line). The filament length L plays the role of a nonaffinity length-scale, i.e. it specifies the length-scale at which medium deformations are inhomogeneous. The filament (with its bending stiffness κ_b) resists the tube deformation, and leads to a frustration effect between filament bending and crosslink deformation. With the possibility of crosslink unbinding ($n_i = 1 \rightarrow 0$) this frustration is avoided. c) The tube potential itself consists of a contribution from the crosslinks (with stiffness k_\times) and from the effective medium k_m . The total deformation \bar{y} is shared between the three elements filament, crosslink and medium, $\bar{y} = y + u_\times + u_m$.

As we want to discuss the role of network deformation on the test filament, we need to know how a macroscopically applied strain field couples to the single filaments. If the effective medium can be thought of as strictly homogeneously elastic then the local strain felt by the filaments would be identical to the macroscopic strain γ imposed by the experimental device. With this assumption of “affine” deformations any network deformation couples to the end-to-end distance of the filament and leads to its extension or compression. Rheological properties are then governed by the resistance of filaments to changes in their end-to-end distance [17, 33, 34, 26].

An alternative point of view is based on the fact, that filaments are anisotropic elastic objects [35], where bending is a much softer deformation mode than stretching ‡. This, together with local structural heterogeneity, may in fact lead to a highly nonaffine

‡ With an effective bending stiffness $k_b \sim \kappa_b/l^3$, and a stretching stiffness $k_s \sim \kappa_b l_p/l^4$ we find $k_b/k_s \sim l/l_p < 1$ as the persistence length l_p is usually much larger than the relevant filament length l .

response where network properties are determined by the resistance of filaments to bending deformations [36, 19, 37, 15, 23].

It has been pointed out in [19] that the filament length L may play the role of a lower cut-off at which the affine assumption breaks down. This breakdown is due to inextensibility and geometric correlations that develop along essentially straight filaments. The actual deformations on the smaller scale of the crosslink (or the mesh-size) then follow from the local network structure. Adopting this latter point of view we assume that macroscopic and homogeneous network deformations (as measured by a strain γ) locally lead to an inhomogeneous distortion of the effective medium that can be accounted for by a strain-dependent tube center line $\bar{y}(s) \propto L\gamma$. The occurrence of the filament length L in this equation is a direct consequence of its role as a nonaffinity length-scale. For our purposes the scaling with L is not decisive, however. What is more important here is that nonaffine deformations of the tube increase with network strain γ and are slaved to the local network structure.

In terms of our discrete crosslinking points this means that one head of the crosslink follows the effective medium deformation at \bar{y}_i , while the second head remains on the filament at y_i . Whenever the filament does not follow the medium, it is the crosslinks that have to deform by $u_\times = \bar{y}_i - y_i$ leading to an elastic energy $k_\times (\bar{y}_i - y_i)^2$. The tube potential is therefore identified with the crosslink deformation energy.

The model thus describes an interplay between crosslink deformation and filament bending. A macroscopic strain applied to the background medium leads to a frustration effect between crosslink and filament deformations. With the possibility of crosslink unbinding, this frustration is avoided. The price to pay is the binding enthalphy $H_{\text{bind}} = -|\mu| \sum_i n_i$, which is assumed to favour the bound crosslink state with $n_i = 1$.

A similar competition between filament and crosslink energies is present in ordered arrays of parallel filaments or filament bundles [38]. In that case, the role of the medium strain is taken by a deformation of the bundle as a whole. This deformation induces filament sliding and leads to a frustration effect between filament stretch and crosslink shear. Subsequently, and to relieve this frustration, a discontinuous crosslink unbinding transition is observed. Interestingly, this has the form of an unzipping transition [39]. Crosslinks unbind first at places where bundle deformation is largest. An interface then moves rapidly to the other end of the bundle.

In the following we will analyze the model defined in equations (1) to (3) with the aim of understanding the combined effects of filament deformation and crosslink binding in response to a network strain. We will discuss some thermodynamic parameters as a function of strain, in particular the average crosslink occupation, $\langle n \rangle$ and the filament energy E . The latter will provide the connection to the stiffness of the network and can be determined in rheological experiments.

3. Monte-Carlo simulations

For the Monte-Carlo simulations we represent the filament by a one-dimensional lattice. To each lattice site ($i = 1, \dots, N_\times$) the pair (y_i, n_i) is attached, denoting the local transverse displacement y_i and the crosslink occupation variables n_i .

As Monte Carlo moves we use single site displacements and crosslink binding/unbinding moves, the latter attempted with ten percent probability. In a displacement move, a lattice site i is selected randomly, and the current displacement y_i of that site is replaced by $y'_i = y_i + \delta$, with $-0.1a < \delta < 0.1a$ drawn uniformly

randomly, and $a = L/N_\times$ is the discretization length, which serves as unit of length here. The new displacement y'_i is accepted with probability $P_{\text{disp}} = \min[1, e^{-\beta\Delta H}]$, where ΔH is the energy difference between initial and final state. During a crosslink move, a bond is selected randomly, and the corresponding occupation variable n_i is flipped ($n_i \rightarrow 1 - n_i$). The new state is accepted with probability $P_{\text{xlink}} = \min[1, e^{-\beta\Delta H + \beta\mu\Delta N}]$, with μ the crosslink chemical potential, $\Delta N = \pm 1$ the change in the number of crosslinks.

In the following we show data where the filament bending stiffness $\kappa_b = 1$ serves as unit of energy. The chemical potential is $|\mu| = 0.001$. The inverse temperature is $\beta = 1000$ such that the persistence length is $l_p = \beta\kappa = 1000$, measured in units of lattice sites a . The filament length is taken to be $L = 20a$, i.e. $N_\times = 20$. For simplicity, we assume the filament to have zero deflection at its ends, $y_0 = y_{N_\times} = 0$. The tube potential is taken as $\bar{y}(s) = \gamma L \sin(qs)$ with $q = \pi/L$, which corresponds to the longest possible wavelength compatible with the chosen boundary conditions.

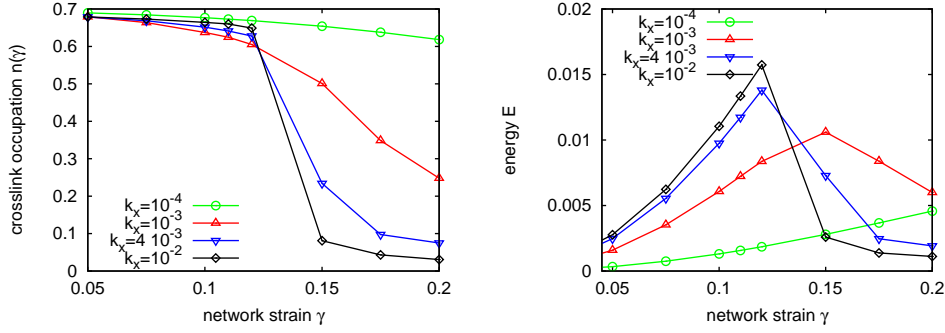


Figure 2. Average crosslink occupation n (left) and elastic energy E (right) as a function of network strain γ and for different crosslink stiffness k_\times . Stiff crosslinks unbind in a sudden discontinuous transition. The elastic energy stored in the filament is lost.

In Fig.2 we monitor the average crosslink occupation $n = \sum_i \langle n_i \rangle / N_\times$ as well as an average energy E , which is obtained by minimizing the total elastic energy for given crosslink occupation. We vary the network strain γ as well as the crosslink stiffness k_\times . It can readily be seen that crosslink stiffness has a dramatic effect on the thermodynamic state of the system.

For mechanically weak crosslinks network strain γ has no strong influence on the binding state. Only few crosslinks unbind upon increasing network deformation. In this regime the crosslinks are not strong enough to enforce filament bending. The elastic energy is small, and primarily stored in the crosslinks. As a consequence, the energy of the bound state is raised and the statistical weight is shifted towards the unbound state. This is the regime discussed in [25, 26, 27] in the context of filamin-crosslinked f-actin networks. Note, that in that model no crosslink unbinding is accounted for. The crosslinks are modeled as nonlinear elastic elements, leading to significant stiffening of the network under strain. We have checked that incorporating nonlinear crosslink compliance in our model reproduces this behavior. Moreover, with the possibility of crosslink unbinding, this stiffening due to crosslink mechanics generally competes with a softening effect due to crosslink unbinding.

When the crosslinks are sufficiently strong, their deformation energy starts to

compete with the filament bending energy. Now crosslinks can force filaments into deformation and the elastic energy is mainly stored in the filaments. At large network strains this energy is too high, however, and unbinding becomes favourable. This is evident as a discontinuous unbinding transition, where nearly all remaining crosslinks unbind simultaneously. Associated with such a transition is a free-energy barrier. The escape time over this barrier sets the time-scale of relaxation of the imposed deformation mode. This will be exponential in the number of crosslinking sites N_\times , reminiscent of what has been proposed in [31].

4. Theoretical framework

Theoretical progress can be made in the continuum limit of equations (1) to (3). Making the mean-field assumption $n_i \rightarrow \sum_i n_i / N_\times \equiv n$, the energy of the test filament can be written as

$$H = \frac{\kappa_b}{2} \int y''(s)^2 ds + \frac{k_\times n}{2a} \int (y(s) - \bar{y}(s))^2 ds. \quad (4)$$

Going to Fourier space, $y(s) = \sum_i y_q \sin(qs)$, the y_q can be integrated out. The resulting effective free energy $F(n)$ can be written as

$$e^{-\beta F(n)} = \left(\prod_q \frac{4\pi/\beta L}{\kappa_b q^4 + k_\times n/a} \right)^{1/2} \exp(-\beta N_\times (F_\gamma(n) + \mu n)) \quad (5)$$

with a deformation-dependent part $F_\gamma(n)$

$$F_\gamma(n) = \sum_q \frac{A_q(\gamma)}{1 + n_q/n} \quad (6)$$

a deformation amplitude $A_q(\gamma) = (a/4)\kappa_b q^4 \bar{y}_q(\gamma)^2$ and the scale for crosslink density $n_q = \kappa_b q^4 a / k_\times$.

The prefactor $(\dots)^{1/2}$ is an entropic contribution that specifies the entropic cost of binding to crosslinks. Clearly, binding suppresses bending undulations and therefore reduces the entropy stored in these modes. The interplay between entropy reduction and μ -dependent enthalpy gain may lead to a thermal unbinding transition [40, 41]. For the case considered here such an unbinding transition is not relevant. Instead, we want to focus on the deformation-dependent part $F_\gamma(n)$.

Just as in the simulations, we make the single-mode assumption, $A_q(\gamma) = A\delta_{qq_1}$ and $q_1 = \pi/L$. Then it is easy to see that the free energy has two saddle-points at $n = 0$ and $n = 1$ and a discontinuous transition between them at $A^* = \mu(1 + n_{q_1})$. This condition gives a critical network strain of $\gamma^* = 0.13$, which compares well with the actual transition as seen in figure 2. This analysis predicts a discontinuous unbinding transition for any value of crosslink stiffness k_\times , in apparent disagreement with the simulations. It turns out that this is a result of the saddle-point approximation. In a more refined treatment, which also includes an ‘‘entropy of mixing’’ term, $p_n = \binom{N_\times}{nN_\times}$, the discontinuous transition is destroyed when the crosslinks are sufficiently soft [38].

Finally, let us comment on the use of the single-mode assumption for the tube center $\bar{y}(s) = \sum_i \bar{y}_q(\gamma) \sin(qs)$. The precise form of $\bar{y}(s)$ and its dependence on network strain γ is, in principle, unknown and one would like to calculate it selfconsistently. As this is unfeasible, one has to rely on assumptions and physical plausibility. Conceptually, the tube deformation in response to network strain γ represents the

missing link between affine deformations on scales larger than the filament length and the actual crosslink motion on the scale of the mesh-size. As such it will be sensitive to the local structure of the network. In [19] it has been shown how such a link can be constructed in terms of local binding angles and the mesh-size distribution.

For our purposes we note, that using one or few higher modes will not fundamentally alter the proposed picture of continuous vs. discontinuous crosslink unbinding. The necessary condition for such a feature to persist is a free energy contribution $F_\gamma(n)$ that grows slower than linear with crosslink occupation n . In this case the linear contribution $-|\mu|n$ from the binding enthalpy will eventually take over.

With one or a finite number of modes present the free energy will eventually saturate $F_\gamma(n) = \text{const.}$ This happens, when the filament is strongly constrained by the crosslinks to precisely follow the tube centerline $y(s) = \bar{y}(s)$. Clearly, binding even more crosslinks cannot lead to a more efficient confinement. A similar result is obtained, if one assumes infinitely many modes, with an amplitude that depends on mode-number as $\bar{y}_q^2 \sim q^{-4}$, i.e. like a thermalized bending mode of a worm-like chain. In this case, the free energy does not saturate but asymptotically grows like $F_\gamma(n) \sim n^{1/4}$, i.e. also slower than linear.

5. Selfconsistent determination of medium stiffness

In the previous sections we assumed the test filament to be coupled to a medium of infinite stiffness. In reality the medium itself is made of crosslinked filaments. Thus the medium properties cannot be set externally, but should be determined self-consistently from the properties of the test filament and its crosslinks. In particular, the studied crosslink unbinding processes reduce the connectivity, and therefore stiffness, of the medium. Unbinding should, therefore, be reflected as a change in the tube potential.

In the following, we will therefore assume the medium to be characterized by an energy function $V_m(u_m)$, which quantifies the energy cost of a deformation u_m . The total tube potential $V = V_m + V_\times$ then contains contributions from both the crosslinks *and* the effective medium. As we expect the medium to be nonlinear, V_m is not necessarily a harmonic function of deformation amplitude.

With a finite medium compliance, any transverse displacements, $\bar{y}_i - y_i$ at a crosslink, has to be shared between the crosslink and the medium, $\bar{y}_i - y_i = u_\times + u_m$. The relative stiffness of the two elements dictate the magnitude of the deformations via a force balance condition [26]. With this the total confinement strength is no longer set by the crosslink stiffness, k_\times , but by an effective stiffness k_{eff} determined by the serial connection of the crosslink and the medium. Unbinding events are expected to reduce the stiffness of the medium and therefore of k_{eff} . In a softer environment, however, the test filament and its crosslinks will have a *reduced* tendency for further crosslink unbinding. There is, therefore, a negative feedback loop between medium stiffness and crosslink unbinding. This may smooth out the sudden unbinding transition that was observed in figure 2.

To calculate V_m we need a condition of self-consistency. This is based on previous approaches [19, 26]. As discussed above, a macroscopic strain γ leads to a local medium deformation of $\bar{y} = \gamma L$. The associated energy cost is given by $V_m(\gamma L)$. At the same time the strain deforms the test filament and its surrounding tube. Therefore, the energy that is needed to impose the strain γ needs to be balanced by the energy E

that is build up in the test filament. This condition can be written in the simple form

$$V_m(\gamma L) = E \quad (7)$$

where $E = \langle H_b + V_\times + V_m \rangle_n$ and the average is taken over crosslink occupation n and network disorder. Despite its simple form, equation (7) is rather difficult to handle, as the unknown potential V_m is required for the evaluation of the statistical average. A possible solution could proceed iteratively, starting from a suitably chosen initial guess. We have not tried such a scheme. Instead, and to make analytical progress, we propose a simplified Ansatz for the confinement potential. As we will see, this Ansatz successfully describes the intuitive result of a softening of the medium as a result of crosslink unbinding.

Let us assume the confinement to be harmonic in the y -degrees of freedom

$$V = \frac{1}{2} \sum n_i k_{\text{eff}} (y_i - \bar{y}_i)^2 \quad (8)$$

but with a confinement strength

$$\frac{1}{k_{\text{eff}}} = \frac{1}{k_\times} + \frac{1}{k_m(\gamma)} \quad (9)$$

that depends on the deformation amplitude γ . The form of equation (9) mimics the serial connection of crosslink and medium.

The energy E can then easily be calculated, and equation (7) takes the simple form

$$k_m = \left\langle L \left(\frac{1}{\kappa q^4} + \frac{a}{n k_{\text{eff}}} \right)^{-1} \right\rangle_n, \quad (10)$$

which has to be solved for $k_m(\gamma)$. The dependence on strain γ is implicit in the averaging procedure, as the tube potential (8) depends on γ . Thus, the effective medium stiffness is obtained as a serial connection of the three mechanical elements fiber, $k_\perp \sim \kappa_b/L^3$, crosslinks, $n k_\times$, and the medium itself, $n k_m$.

Figure 3 presents a graphical solution of equation (10). The symbols give the effective fiber stiffness (right-hand side of the equation, from the MC simulations) plotted as a function of k_{eff} and taken at different deformation amplitudes γ . If we assume k_{eff} to be given and constant (as in figure 2), a vertical line would give us the fiber stiffness as a function of amplitude γ . For k_{eff} large enough (indicated by the vertical dashed line), a discontinuous transition is evident in the data. To extract the actual network modulus $k_m(\gamma)$ we have to find the intersection with the curve $k_m(k_{\text{eff}})$, equation (9), which is drawn as solid black line. The resulting k_m is clearly decreasing with deformation amplitude, however, the discontinuous nature is not obvious anymore.

A quantitative analysis is presented in figure 4. The resulting network modulus $k_m(\gamma)$ is plotted for different crosslink stiffness k_\times . For small strain the modulus k_m is constant, as for a linear elastic material. This linear stiffness first increases with crosslink stiffness but then saturates, when the crosslinks become stiffer than the fiber. This behavior is in line with the serial connection between fiber, crosslink and medium as embodied in equation (10). In a serial connection it is always the softer element that governs the mechanical properties.

At higher strain and for stiff crosslinks, the network modulus k_m decreases. This decrease is not discontinuous as expected from figure 2, but rather smooth and gradual.

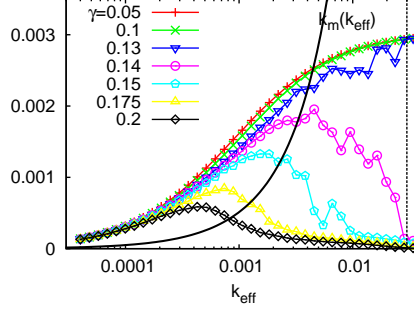


Figure 3. Graphical solution to equation (10) for $k_x = 0.04$. The right-hand side of the equation (symbols) is drawn for different deformation amplitudes γ . The network modulus k_m is found by intersecting with the left-hand side of the equation (solid line), $k_m(k_{\text{eff}})$. The vertical dashed line corresponds to the solution without the self-consistency condition, i.e. with a prescribed medium stiffness, as discussed in section 3.

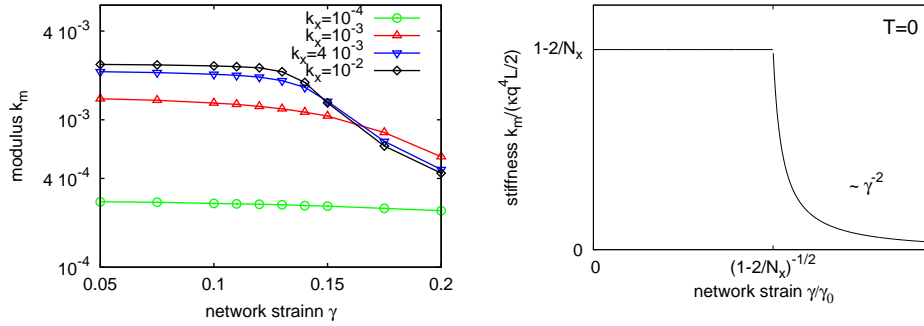


Figure 4. (left) Network modulus $k_m(\gamma)$ for different crosslink stiffness k_x as obtained from the MC simulation. (right) Analytical result for $k_x = \infty$ and based on the zero temperature approximation presented in section 4.

In fact, a zero-temperature analysis along the lines of section 4 shows that the discontinuity turns into a second-order transition, with a cusp as indicated in the right panel of figure 4. In the limit, $k_x \rightarrow \infty$, we find

$$k_m(\gamma) = \frac{\kappa q^4 L}{2} \cdot \begin{cases} (1 - 2/N_x) & \text{for } \gamma < \gamma^* \\ \frac{2/N_x}{(\gamma/\gamma_0)^2 - 1} & \text{for } \gamma \geq \gamma^* \end{cases} \quad (11)$$

with $\gamma_0^2 = 4\mu/\kappa q^4 L^2 a$ and the critical amplitude $\gamma^* = \gamma_0(1 - 2/N_x)^{-1/2}$.

Finally, figure 5 shows the resulting crosslink occupation n as well as the average energy of the test filament. Qualitatively, the conclusion is similar as in figure 2. The crosslink stiffness is identified as key factor in mediating crosslink unbinding processes. Quantitatively, we see that the unbinding under load is more gradual in this second scenario, where the medium stiffness is determined self-consistently. This reflects the anticipated negative feedback of medium stiffness on crosslink unbinding.

Looking back at figure 3 it is clear that the strength of the variation in k_m or n depends on the relative location of the two curves, $k_m(k_{\text{eff}})$ and the effective fiber stiffness as embodied in the right-hand side of equation (10). For this geometrical factors could be important. These could arise from network structural randomness, like bond angles or crosslink distances. In our calculation these geometrical factors have been disregarded, which corresponds to a regular network architecture.

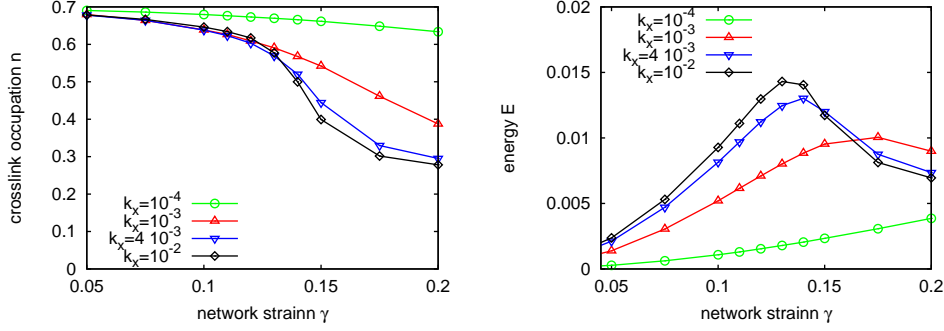


Figure 5. Average crosslink occupation n (left) and elastic energy E (right) as a function of network strain γ and for various crosslink stiffness k_x . Stiff crosslinks tend to unbind under strain leading to an associated reduction in elastic energy. As compared to figure 2, however, unbinding is not dramatically discontinuous but rather smooth.

6. Conclusion

In this study, we discussed the interplay between filament and crosslink elasticity in semiflexible polymer networks. In particular, we were interested in the force-induced unbinding of crosslinks in response to external load. Importantly, we considered the limiting case of slowly changing load (“quasistatic”), where the system is given time enough to reach an equilibrium state at each load level. The model presented is therefore purely thermodynamic in nature, and no rate constants for the crosslink dynamics are needed. Possible extensions of the present work may include the effect of a load applied at finite rates.

We model the filament network as an elastic medium with modulus k_m . The stiffness is calculated on a self-consistent basis from the response of a test filament that is embedded into the medium. On the microscopic level the effect of the network is to confine the filament to a tube-like region in space.

We quantify the applied load in terms of a network strain γ , which is homogeneous on a macroscopic scale. On the local scale of the individual filaments, however, even a homogeneous strain leads to an inhomogeneous (“nonaffine”) deformation of the effective medium. This is a natural consequence of network heterogeneity and filament mechanical anisotropy. We modeled this inhomogeneous deformation in terms of a distortion of the center-line of the confinement tube of the filaments. The filament (with its bending stiffness κ_b) resists this tube deformation, which leads to a frustration effect between filament bending, crosslink deformation and medium deformation.

This competition is formalized in equation (10) which we rewrite here as

$$k_m = \left\langle \left[\frac{1}{k_\perp} + \frac{1}{Nk_\times} + \frac{1}{Nk_m} \right]^{-1} \right\rangle_N. \quad (12)$$

with an effective filament bending stiffness $k_\perp \sim \kappa_b/L^3$, the crosslink stiffness k_\times and the network modulus k_m . By solving this equation, the latter is thereby obtained self-consistently from a serial connection of the filament, the crosslinks and the medium itself. The most interesting feature in this equation is the dependence on the number of bound crosslinks N . With the possibility of crosslink unbinding (decreasing N) the competition between the different mechanical elements is avoided. This leads to a reduction of the medium stiffness with increasing network strain, and eventually to network failure, when all crosslinks are unbound.

Different scenarios can be distinguished. If the crosslinks are soft (k_\times small), then the network modulus is dominated by the crosslinks, $k_m \sim k_\times$, and the filament effectively behaves as a rigid rod. The tendency for crosslink unbinding is weak as it does not lead to a significant stress relaxation. On the other hand, if crosslink and filament stiffness compete (k_\times large), then unbinding events do help relax the imposed stress and reduce the amount of stored energy. This unbinding can be sudden and discontinuous or take the form of a second-order transition, where $k_m(\gamma)$ or $N(\gamma)$ display a kink at a critical load γ^* .

Experimentally, strain-induced stress relaxation is observed in living cells after transient pulses of stretch [5] or in-vitro when the loading rates are small [9]. For larger loading rates, a pronounced stiffening is found in the in-vitro system. This is consistent with the first-order crosslink unbinding scenario discussed here. In this picture, a free-energy barrier, and the associated time-scale, prevents crosslink unbinding when the loading rate is too large. Related phenomena are important for the aging behavior of kinetically trapped actin networks [30], where built in stresses only relax slowly and by the action of crosslink binding events. Similarly, red blood cells owe their remarkable ability to undergo reversible shape changes to a rewiring of the spectrin network [42, 44].

This work goes beyond previous models in considering both the filament and the crosslink stiffness as factors for the rheological properties of crosslinked filament networks. Moreover, we show how this interplay affects the tendency of crosslinks to bind/unbind from the filaments during a rheological experiment. The strain field imposed by the rheometer leads to nonaffine deformations on the scale of the filaments. As compared to previous models, the unrealistic assumption of affine deformations is abandoned in favour of a model that incorporates the filament length as the fundamental non-affinity scale.

In extensions of the present model one should incorporate nonlinear elastic compliances of the filaments and of the crosslinks. This is believed to be important for the nonlinear strain stiffening of f-actin networks. The complex interplay between stiffening and softening described in rheological experiments [9] would then reflect the relative importance of filament/crosslink elasticity, which lead to stiffening, and softening as due to crosslink unbinding. Interestingly, unbinding processes may under some conditions also lead to the reverse (i.e. stiffening) effect [43]. This further contributes to the rich nonlinear behavior of these systems, which is far from being fully understood.

Acknowledgments

Support by the Deutsche Forschungsgemeinschaft, Emmy Noether program: He 6322/1-1, and by the collaborative research center SFB 937 is acknowledged.

References

- [1] D. A. Fletcher and D. Mullins. Cell mechanics and the cytoskeleton. *Nature*, 463:485, 2010.
- [2] B. D. Hoffman and J. C. Crocker. Cell mechanics: Dissecting the physical responses of cells to force. *Ann. Rev. Biomed. Eng.*, 11:259, 2009.
- [3] Q. Wen and P.A. Janmey. Polymer physics of the cytoskeleton. *CURRENT OPINION IN SOLID STATE AND MATERIALS SCIENCE*, 15:177, 2011.
- [4] Philip Kollmannsberger and Ben Fabry. Linear and nonlinear rheology of living cells. *Annual Review of Materials Research*, 41(1):75–97, 2011.
- [5] X. Trepate, L. Deng, S. S. An, D. Navajas, D. J. Tschumperlin, W. T. Gerthoffer, J. P. Butler, and J. J. Fredberg. Universal physical responses to stretch in the living cell. *Nature*, 447:592, 2007.
- [6] Pablo Fernandez, Pramod A. Pullarkat, and Albrecht Ott. A master relation defines the nonlinear viscoelasticity of single fibroblasts. *Biophysical Journal*, 90(10):3796 – 3805, 2006.
- [7] Lars Wolff, Pablo Fernandez, and Klaus Kroy. Inelastic mechanics of sticky biopolymer networks. *New Journal of Physics*, 12(5):053024, 2010.
- [8] A. Bausch and K. Kroy. Cytoskeleton from the assembly line: a bottom-up approach to cell mechanics. *Nature Physics*, 2:231, 2006.
- [9] O. Lieleg, M. M. A. E. Claessens, and Andreas R. Bausch. Structure and dynamics of cross-linked actin networks. *Soft Matter*, 6:218, 2010.
- [10] K. E. Kasza, A. C. Rowat, J. Liu, T. E. Angelini, C. P. Brangwynne, G. H. Koenderink, and D. A. Weitz. The cell as a material. *Curr. Op. Cell. Biol.*, 19:101, 2007.
- [11] G. H. Koenderink, M. Atakhorrami, F. C. MacKintosh, and C. F. Schmidt. High-frequency stress relaxation in semiflexible polymer solutions and networks. *Phys. Rev. Lett.*, 96:138307, 2006.
- [12] M. L. Gardel, J. H. Shin, F. C. MacKintosh, L. Mahadevan, P. A. Matsudaira, and D. A. Weitz. *Science*, 304:1301, 2004.
- [13] J. Liu, G. H. Koenderink, K. E. Kasza, F. C. MacKintosh, and D. A. Weitz. Visualizing the strain field in semiflexible polymer networks: Strain fluctuations and nonlinear rheology of *f*-actin gels. *Phys. Rev. Lett.*, 98:198304, May 2007.
- [14] Q. Wen, A. Basu, J. P. Winer, A. Yodh, and P. A. Janmey. Local and global deformations in a strain-stiffening fibrin gel. *New J. Physics*, 9:428, 2007.
- [15] O. Lieleg, M. Claessens, C. Heussinger, E. Frey, and A. R. Bausch. Mechanics of bundled semiflexible polymer networks. *Phys. Rev. Lett.*, 99:088102, 2007.
- [16] M. L. Gardel, J. H. Shin, F. C. MacKintosh, L. Mahadevan, P. A. Matsudaira, and D. A. Weitz. *Phys. Rev. Lett.*, 93:188102, 2004.
- [17] F. C. MacKintosh, J. Käs, and P. A. Janmey. *Phys. Rev. Lett.*, 75:4425, 1995.
- [18] F. Gittes and F. C. MacKintosh. Dynamic shear modulus of a semiflexible polymer network. *Phys. Rev. E*, 58:R1241, 1998.
- [19] C. Heussinger, B. Schaefer, and E. Frey. Nonaffine rubber elasticity for stiff polymer networks. *Phys. Rev. E*, 76:031906, 2007.
- [20] J. Wilhelm and E. Frey. *Phys. Rev. Lett.*, 91:108103, 2003.
- [21] D. A. Head, A. J. Levine, and F. C. MacKintosh. *Phys. Rev. Lett.*, 91:108102, 2003.
- [22] C. Heussinger and E. Frey. Stiff polymers, foams, and fiber networks. *Phys. Rev. Lett.*, 96:17802, 2006.
- [23] P R Onck, T Koeman, T van Dillen, and E van der Giessen. Alternative explanation of stiffening in cross-linked semiflexible networks. *Phys Rev Lett*, 95:178102, 2005.
- [24] E. M. Huisman, C. Storm, and G. T. Barkema. Frequency-dependent stiffening of semiflexible networks: A dynamical nonaffine to affine transition. *Phys. Rev. E*, 82:061902, Dec 2010.
- [25] C. P. Broedersz, C. Storm, and F. C. MacKintosh. Nonlinear elasticity of composite networks of stiff biopolymers with flexible linkers. *Phys. Rev. Lett.*, 101:118103, Sep 2008.
- [26] C. P. Broedersz, C. Storm, and F. C. MacKintosh. Effective-medium approach for stiff polymer networks with flexible cross-links. *Phys. Rev. E*, 79:061914, Jun 2009.
- [27] K.E. Kasza, C.P. Broedersz, G.H. Koenderink, Y.C. Lin, W. Messner, E.A. Millman,

- F. Nakamura, , T.P. Stossel, F.C. MacKintosh, and D.A. Weitz. Actin filament length tunes elasticity of flexibly cross-linked actin networks. *Biophys. J.*, 99:1091, 2010.
- [28] O. Lieleg, M. M. A. E. Claessens, Y. Luan, and A. R. Bausch. Transient binding and dissipation in cross-linked actin networks. *Phys. Rev. Lett.*, 101(10):108101, Sep 2008.
- [29] Chase P. Broedersz, Martin Depken, Norman Y. Yao, Martin R. Pollak, David A. Weitz, and Frederick C. MacKintosh. Cross-link-governed dynamics of biopolymer networks. *Phys. Rev. Lett.*, 105:238101, Nov 2010.
- [30] O. Lieleg, J. Kayser, G. Brambilla, L. Cipelletti, and A. R. Bausch. Slow dynamics and internal stress relaxation in bundled cytoskeletal networks. *Nat. Mat.*, 10:236, 2011.
- [31] K. Kroy and J. Glaser. The glassy wormlike chain. *New J. Phys.*, 9:416, 2007.
- [32] Christine Semmrich, Tobias Storz, Jens Glaser, Rudolf Merkel, Andreas R. Bausch, and Klaus Kroy. Glass transition and rheological redundancy in f-actin solutions. *Proceedings of the National Academy of Sciences*, 104(51):20199–20203, 2007.
- [33] C. Storm, J. J. Pastore, F. C. MacKintosh, T. C. Lubensky, and P. A. Janmey. Nonlinear elasticity in biological gels. *Nature*, 435(7039):191–194, 2005.
- [34] M. L. Gardel, J. H. Shin, , F. C. MacKintosh, L. Mahadevan, P. Matsudaira, and D. A. Weitz. Elastic behavior of cross-linked and bundled actin networks. *Science*, 304(5675):1301–1305, 2004.
- [35] K. Kroy and E. Frey. Force-extension relation and plateau modulus for wormlike chains. *Physical Review Letters*, 77(2), 1996.
- [36] C. Heussinger and E. Frey. Floppy modes and non-affine deformations in random fiber networks. *Phys. Rev. Lett.*, 97:105501, 2006.
- [37] C. Heussinger and E. Frey. Force distributions and force chains in random stiff fiber networks. *Eur. Phys. J. E*, 24:47, 2007.
- [38] Claus Heussinger. Cooperative crosslink (un)binding in slowly driven bundles of semiflexible filaments. *Phys. Rev. E*, 83:050902, May 2011.
- [39] R.L.C. Vink and C. Heussinger. Cross-linked biopolymer bundles: Cross-link reversibility leads to cooperative binding/unbinding phenomena. *J. Chem. Phys.*, 136:035102, 2012.
- [40] J. Kierfeld, T. Kühne, and R. Lipowsky. Discontinuous unbinding transition of filament bundles. *Phys. Rev. Lett.*, 95:038102, 2005.
- [41] P. Benetatos and E. Frey. Depinning of semiflexible polymers. *Phys. Rev. E*, 67(5):051108, May 2003.
- [42] N. S. Gov. Active elastic network: Cytoskeleton of the red blood cell. *Phys. Rev. E*, 75:011921, 2007.
- [43] N. S. Gov. Less is more: removing membrane attachments stiffens the RBC cytoskeleton. *New J. Phys.*, 9:429, 2007.
- [44] J. Li, G. Lykotrafitis, M. Dao and S. Suresh. Cytoskeletal dynamics of human erythrocyte. *Proc. Natl. Acad. Sci. USA*, 104:4937, 2007.